Generic suppression of conductance quantization of interacting electrons in graphene nanoribbons in a perpendicular magnetic field

A. A. Shylau* and I. V. Zozoulenko†
Solid State Electronics, ITN, Linköping University, 601 74, Norrköping, Sweden

H. Xu and T. Heinzel
Condensed Matter Physics Laboratory, Heinrich-Heine-Universität, Universitätsstr.1, 40225 Düsseldorf, Germany
(Dated: July 26, 2010)

The effects of electron interaction on the magnetoconductance of graphene nanoribbons (GNRs) are studied within the Hartree approximation. We find that a perpendicular magnetic field leads to a suppression instead of an expected improvement of the quantization. This suppression is traced back to interaction-induced modifications of the band structure leading to the formation of compressible strips in the middle of GNRs. It is also shown that the hard wall confinement combined with electron interaction generates overlaps between forward and backward propagating states, which may significantly enhance backscattering in realistic GNRs. The relation to available experiments is discussed.

PACS numbers: 72.80.Vp, 73.22.Pr, 73.63.Nm, 73.43.-f

Conductance quantization in quantum point contacts (QPCs) and quantum wires represents a hallmark of mesoscopic physics [1, 2]. At zero magnetic field this effect can be understood within a noninteracting electron picture as quantization of the transverse electron motion where, according to the Landauer-Buttiker formalism, each propagating mode contributes with the conductance quantum $G_0 = 2e^2/h$ to the total conductance [1, 2]. In a perpendicular magnetic field B the propagating states acquire qualitatively new features gradually transforming into edge states as B is increased [2–5]. Since the left- and right-propagating edge states get localized in transverse direction at opposite wire edges in sufficiently strong magnetic fields, the coupling between them can be exponentially small. This, in turn, leads to a strongly suppressed backscattering and hence to a drastic improvement of the conductance quantization[2–6]. Taking electron interaction and screening in high magnetic fields into account leads to new features such as formation of compressible and incompressible strips[7], which are essential for an interpretation of various magnetotransport phenomena in conventional QPCs and quantum wires defined in two-dimensional electron gases (2DEGs) [7, 8].

The isolation of graphene[9] has immediately inspired the search for conductance quantization in graphene nanoribbons (GNRs). However, in all experiments reported so far conductance quantization at $B = 0$ is absent [10] or strongly suppressed [11], which by now is well understood and attributed to the effects of impurity scattering and/or edge disorder [12]. In analogy with conventional QPC structures one would thus anticipate a drastic improvement of the conductance quantization in GNRs in the edge state regime due to the expected suppression of backscattering [4]. Surprisingly enough, the magnetoconductance measurements on GNRs reported so far show no evidence of the expected improvement of the conductance quantization [13, 14]. Even relatively large graphene strips ($\gtrsim 1\mu$m) [15, 16] do not exhibit quantization plateaus at high magnetic fields of high quality as routinely seen in corresponding conventional heterostructures [6].

In the present paper we study the magnetoconductance of GNRs taking electron interaction on the Hartree level into account. Contrary to expectations based on the conventional edge-state picture of noninteracting electrons [4] we find that application of a magnetic field leads to a *suppression* instead of expected improvement of the conductance quantization. This behavior is related to a drastic modification of the GNR band structure by electron interaction leading, in particular, to the formation of compressible strips in the middle of the ribbon. These features are generic in GNRs, but in contrast to most of the distinct properties of graphene [18] they are not caused by the Dirac-like energy dispersion but rather by the hard-wall confinement.

We consider a GNR attached to semi-infinitive leads acting as electron reservoirs and subjected to a perpendicular magnetic field B, see inset to Fig. 1. The ribbon of width $w = 50$ nm resides on top of a SiO_2 insulating substrate ($\varepsilon_r = 3.9$) of thickness $d = 300$ nm, below which a metallic gate is located. The system is described by the standard p-orbital tight-binding Hamiltonian[18, 19]

$$H = \sum_{\mathbf{r}} V_H(\mathbf{r}) a_{\mathbf{r}}^+ a_{\mathbf{r}} - \sum_{\mathbf{r},\Delta} t_{\mathbf{r},\mathbf{r}+\Delta} a_{\mathbf{r}}^+ a_{\mathbf{r}+\Delta}, \qquad (1)$$

where the summation runs over all sites of the graphene lattice, Δ includes the nearest neighbors only, $t_{\mathbf{r},\mathbf{r}+\Delta} = t_0 \exp(i2\pi\phi_{\mathbf{r},\mathbf{r}+\Delta}/\phi_0)$ with $t_0 = 2.77$ eV, $\phi_0 = h/e$ being the magnetic flux quantum and $\phi_{\mathbf{r},\mathbf{r}+\Delta} = \int_{\mathbf{r}}^{\mathbf{r}+\Delta} \mathbf{A} \cdot d\mathbf{l}$ with $\mathbf{A}$ being the vector potential. We use the Landau gauge, $\mathbf{A} = (-By, 0)$. The interaction among the extra

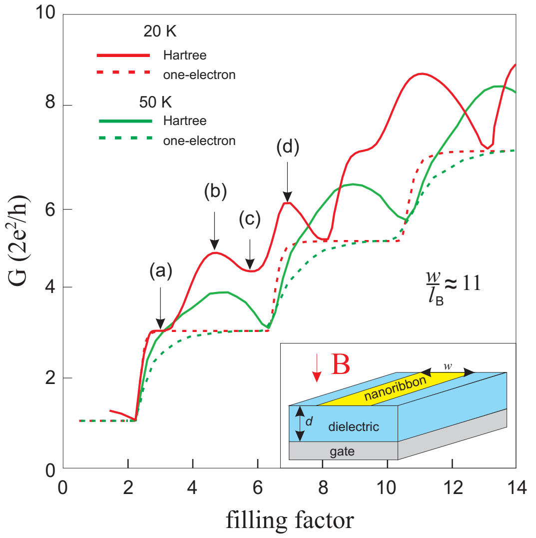

FIG. 1: (Color online) Conductance of the GNR as a function of filling factor for interacting and noninteracting electrons at temperatures $T = 20$ K and 50 K in a magnetic field B=30 T (corresponding to $l_B/w \approx 11$). The arrows indicate the filling factors for which the corresponding band structures are shown in Fig. (2) . Inset: sketch of the sample geometry. An armchair GNR of width $w = 50$ nm is located on top of an insulating SiO_2 layer ($\varepsilon_r = 3.9$, thickness $d = 300$ nm) and a gate electrode.

charges of the density $n(\mathbf{r})$ is described within Hartree approximation

$$V_H(\mathbf{r}) = \frac{e^2}{4\pi\varepsilon_0\varepsilon_r} \sum_{\mathbf{r}' \neq \mathbf{r}} n(\mathbf{r}') \left(\frac{1}{|\mathbf{r}-\mathbf{r}'|} - \frac{1}{\sqrt{|\mathbf{r}-\mathbf{r}'|^2 + 4d^2}} \right) \tag{2}$$

where the first term describes electron interaction within the ribbon while the second term takes the presence of the metallic gate on the basis of the image charge method into account. The band structure, the potential profile, the charge density distribution are calculated self-consistently using the Green's function technique (see Refs. [20, 21] for details). The magnetoconductance through the nanoribbon in the linear response regime is given by the Landauer formula

$$G(E_F, B) = \frac{2e^2}{h} \int T(E, B) \left[-\frac{\partial f_{FD}(E - E_F)}{\partial E} \right] dE \tag{3}$$

where $f_{FD}(E-E_F)$ is the Fermi-Dirac distribution function and E_F denotes the Fermi energy. For an ideal system (without scattering), the total transmission coefficient $T(E, B)$ is equal to the number of propagating states, $T(E, B) = N_{prop}$, such that the conductance is simply proportional to N_{prop} weighted by $\frac{\partial f_{FD}}{\partial E}$ which is different from zero in an energy window $\sim 4\pi k_B T$.

Figure 1 shows the conductance of the ideal nanoribbon for a representative magnetic field $B = 30$ T as a function of the filling factor $\nu = \langle n \rangle \phi_0 / B$ for two representative temperatures, with $\langle n \rangle$ being the electron density averaged across the ribbon. Here, ν is tuned by varying the gate voltage V_g which is applied vs. the grounded nanoribbon and thus tunes the electron density. The ratio of GNR width to magnetic length, $w/l_B \approx 11$, is chosen in accordance with typical experiments [13, 14]. It is important to emphasize that the obtained results remain practically unchanged when the system is scaled by, e.g. increasing w while simultaneously reducing B such that the ratio w/l_B remains constant. In order to highlight the role of electron interaction, we compare our self-consistent calculations with a noninteracting picture. The calculated conductance shows a striking difference between the interacting and noninteracting cases. First of all, at a given filling factor, the conductance of the interacting system is always larger than that one of the corresponding noninteracting system. Second, the perfect quantization steps calculated for the noninteracting picture are destroyed as the interaction is turned on, and the conductance develops pronounced bump-like features. Note that the elevated temperature smears the conductance bumps to some extent, but they still dominate the conductance even at $T = 50K$. We also note that we performed the magnetotransport calculations for a high-k material ($\varepsilon_r = 47$) and a gate closeby, $d = 5$ nm when the electron interaction is strongly screened (not shown here). We find that even in this case the bumps are suppressed but still clearly dominate the conductance.

We proceed by interpreting the suppression of conductance plateaux in terms of interaction-induced modifications of the energy dispersion. The evolution of the band structure as a function of ν in the interval covering a representative bump, $2.9 \lesssim \nu \lesssim 5.7$ (corresponding to arrows (a)-(c) in Fig. 1) is presented in Fig. 2 both for interacting and non-interacting cases. The dispersion relation for non-interacting electrons shows flat regions corresponding to the Landau levels in bulk graphene[18, 23] and dispersiveness states close to the GNR's boundaries representing familiar edge states [5]. Note that the position and the number of propagating states at a given energy are determined by the intersection of the Fermi energy level with the corresponding subbands.

For non-interacting electrons changing the gate voltage results in a shift of the Fermi level but does not modify the subband structure. Qualitatively new features arise when the electron interaction is taken into account. One of the most distinct features is that the dispersionless state in the center of the GNR (corresponding to the 1st Landau level (LL)) gets pinned to the Fermi energy thus forming a compressible strip. These strips are marked in yellow in Fig. 2 (b)-(d); following Suzuki and Ando [24] we define a compressible strip as a region where the dispersion lies within the energy window $|E-E_F| < 2\pi k_B T$. The compressible strips form because in the above energy window the states are partially filled (i.e. $0 < f_{FD} < 1$)

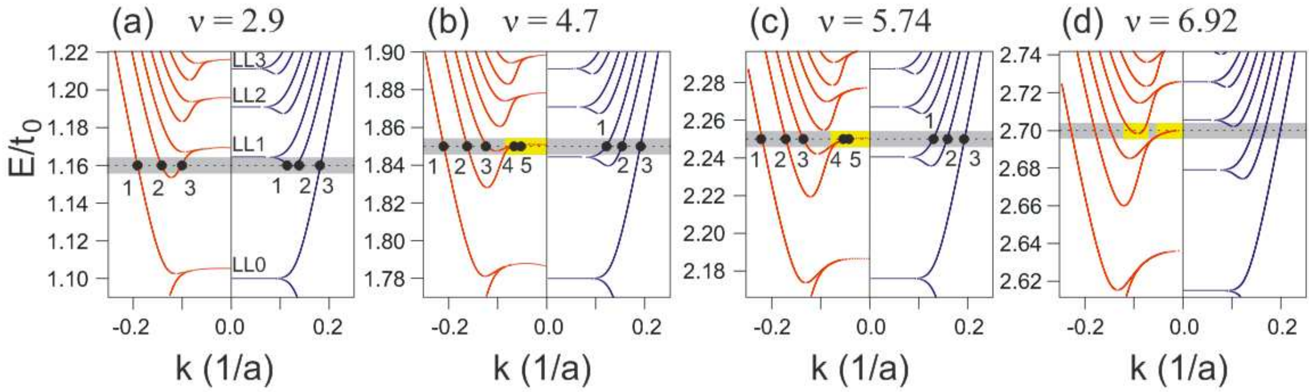

FIG. 2: (Color online) Evolution of the band structure of the GNR at different filling factors corresponding to arrows (a) - (d) in Fig. 1. Left and right parts of the panels correspond to the interacting and non-interacting case, respectively. In order to align noninteracting and Hartree bands the one-electron dispersions have been shifted along the energy axis by the average Hartree energy. Gray fields mark the energy window $[E_F - 2\pi k_b T, E_F + 2\pi k_b T]$; yellow fields mark the compressible strips. The dotted line shows E_F. The black full circles mark the intersections of the Fermi level with the dispersion curves, thereby identifying the propagating states at E_F. In (a) the dispersionless states are marked according to the corresponding Landau levels (LL) of the bulk graphene.

and hence the system has a metallic character. Due to the metallic behavior, the electron density can easily be redistributed in order to effectively screen the external potential [7]. The compressible strips can form only if the confining potential is sufficiently smooth [7]. The GNRs have a hard-wall confinement and hence the compressible strips can form only in the center but not for the edge states. Note that the existence of compressible strips in graphene has been recently demonstrated by Silvestrov *et al.*[22].

Because of the pinning of the LL to the Fermi energy, changing of the filling factor leads to a significant distortion of the dispersion curves. For a given B, the larger the gate voltage (and therefore ν) is, the stronger the bands are distorted in comparison to the noninteracting picture (c.f. (a)-(d) in Fig. 2). This distortion eventually leads to the bumps in the conductance. Indeed, according to Eq. (3) the conductance is given by the number of propagating states averaged in the energy window $|E - E_F| < 2k_B T$. For noninteracting electrons the dispersion relation is not changed as ν is varied and the number of propagating states remains always the same, $N_{prop} = 3$ (see right panels in Fig. 2 (a)-(c)). This, according to Eq. (3), leads to a conductance plateau $G = 3G_0$. In contrast, for interacting electrons the dispersion relation gets distorted and there is always an energy interval in the window $|E - E_F| < 2k_B T$ where the number of propagating states exceeds that for the noninteracting case. This is illustrated in the left panels in Fig. 2 (b)-(c) for $E = E_F$ where $N_{prop} = 5$. As a result, the conductance exceeds its noninteracting value of $3G_0$ exhibiting the pronounced bumps.

With further increase of ν, the compressible strips pinned to the Fermi level form not only in the center of the strip, but further away from the center (as illustrated in Fig. 2 (d)). Note that the second compressible strip in Fig. 2 (d) leads to the formation of a bump in the conductance in the region $6 \lesssim \nu \lesssim 9$.

Let us now discuss in detail a structure of propagating states of the interacting electrons in GNRs. Figures 3 (a), (b) show the electron density and the confining potential for a representative filling factor $\nu = 4.7$ [(b)-arrow on Fig. (1)]. The distribution of charge density is highly nonuniform showing charge accumulation at the boundaries [21, 22]. There are two types of states, which have a different microscopic character. The first type [1,2,3 states in (a)-(c)] corresponds to edge states propagating near the boundaries and have the same structure for interacting and noninteracting cases. The second type [states 4 and 5] corresponds to the states which form compressible strips in the center of the ribbon as discussed above. The most prominent feature of these states is that their direction of propagation is opposite to that one of the edge states residing in the same half of the GNR. This is in contract to the noninteracting picture, where due to the presence of a magnetic field, forward and backward propagating states are localized at different boundaries by Lorentz forces. This unusual behavior can be interpreted in terms of a semiclassical analogue. The electrons scattered at the boundaries are described by skipping orbits. Besides the hard-wall potential walls provided by nanoribbon's edges, there are two additional walls originating from the self-consistent potential which, together with the outer walls of the GNR, form triangular quantum wells at the ribbon's edges [Fig. 3 (b)]. Electrons which strike the left side of the right triangular quantum well propagate in the same direction as the electrons that strike the left edge of the nanoribbon as schematically il-

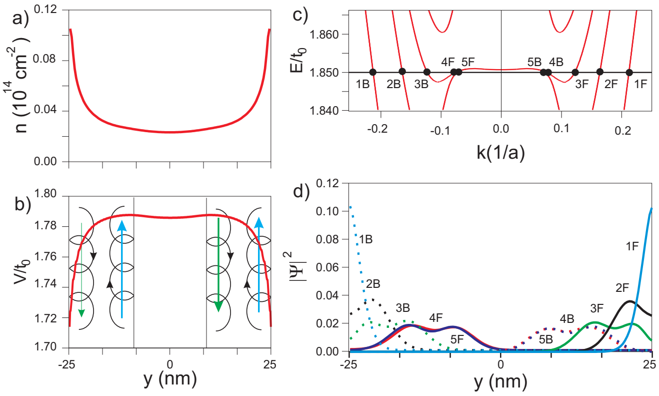

FIG. 3: (Color online) (a) Electron concentration $n(y)$, (b) self-consistent potential V_H across the GNR, and (c) the band structure at $\nu = 4.7$. (d) The square modulus of the wave functions at E_F of forward (F) and backward (B) propagating states (solid and dashed lines correspondingly) marked in (c). For the sake of clarity the electron densities, potential and the wave functions are averaged over two adjacent slices and 3 adjacent sites of the same slice). Inset in (b) illustrates classical skipping orbits.

lustrated in Fig. 3 (b).

This feature of propagating states in high magnetic field makes GNRs much more sensitive to the effect of the disorder in comparison to conventional split-gate structures defined in 2DEG. Indeed, for interacting electrons in GNRs the overlap between the backward (4B, 5B) and forward (1F-3F) propagating states is significant. In realistic GNRs with disorder this would result in a strong enhancement of backscattering, which, in turn, can lead to a further distortion of the conductance (in addition to bumps that are present even in ideal GNRs without disorder).

Note that the features of the band structure and character of propagating states in GNRs discussed above are not caused by the Dirac-like energy dispersion but rather by the hard-wall confinement at the boundaries. These features of the GNRs resemble corresponding features of cleaved-edge overgrown (CEO) quantum wires [17] that also have a hard-wall confinement. We therefore expect that magnetoconductance of CEO also should exhibit suppressed quantization of high field (Note that we were not able to find any reports on magnetoconductance measurements in CEO wires at high magnetic field).

We continue by relating our results to the available experimental data. We are not aware of any studies reporting a drastic improvement of the conductance quantization in GNRs by perpendicular magnetic field. The observed conductance in narrow GNRs exhibit irregular [14] or bump-like features [13], and the wider structures show pronounced bumps superimposed on conductance plateaus [15, 16]. Even though this is consistent with our findings, this can hardly be regarded as a definite experimental validation of our predictions. We thus hope that our work will motivate systematic studies of the magnetoconductance that will shed new light on properties of interacting electrons in confined graphene systems.

In conclusion, we have shown that applying a perpendicular magnetic field to a GNR containing an interaction electron gas leads to a *suppression* instead of expected improvement of conductance quantization. This surprising behavior is related to the modification of the band structure of the GNR due to the electron interaction leading, in particular, to the formation of compressible strips in the middle of the ribbon and existence of counter-propagating states in the same half of the GNR.

A.A.S. and I. V. Z acknowledge a support of the Swedish Research Council (VR).

* Electronic address: artsh@itn.liu.se
† Electronic address: igozo@itn.liu.se

[1] B. J. van Wees, *et al.*, Phys. Rev. Lett. **60**, 848 (1988); D. A. Wharam, *et al.*, J. Phys. C: Solid State Phys. **21**, L209 (1988).
[2] C.W. J. Beenakker and H. van Houten, Solid State Physics **44**, 1 (1991).
[3] B. I. Halperin, Phys. Rev. B **25**, 2185 (1982); P. Streda, J. Kucera, and A. H. MacDonald, Phys. Rev. Lett. **59**, 1973 (1987).
[4] M. Buttiker, Phys. Bev. B **38**, 9375 (1988).
[5] J. Davies, *The Physics of Low-Dimensional Semiconductors* (Cambridge University Press, Cambridge, 1998).
[6] B. J. van Wees *et al.*, Phys. Rev. B **43**, 12431(1991).
[7] D. B. Chklovskii, B. I. Shklovskii, and L. I. Glazman, Phys. Rev. B **46**, 4026 (1992); D. B. Chklovskii, K. A. Matveev, and B. I. Shklovskii, *ibid.* **47**, 12605 (1993).
[8] S. Ihnatsenka and I. V. Zozoulenko, Phys. Rev. B **78**, 035340 (2008).
[9] K. S. Novoselov *et al.* Science **306**, 666 (2004).
[10] M. Y. Han *et al.*, Phys. Rev. Lett. **98**, 206805 (2007).
[11] Y.-M. Lin *et al.* Phys. Rev. B **78**, 161409 (2008).
[12] M. Evaldsson *et al.*, Phys. Rev. B **78**, 161407 (2008); E. R. Mucciolo, A. H. Castro Neto, and C. H. Lewenkopf, Phys. Rev. B **79**, 075407 (2009); S. Ihnatsenka and G. Kirczenow, Phys. Rev. B **80**, 201407 (2009).
[13] F. Molitor *et al.*, Phys. Rev. B **79**, 075426 (2009).
[14] J. B. Oostinga, B. Sacepe, M.F. Craciun, A.F. Morpurgo, Phys. Rev. B **81**, 193408 (2010).
[15] J. R. Williams *et al.*, Phys. Rev. B **80**, 045408 (2009).
[16] X. Du *et al.*, Nature **462**, 196 (2009); K. I. Bolotin *et al.*, Nature **462**, 196 (2009).
[17] S. Ihnatsenka and I. V. Zozoulenko, Phys. Rev. B **74**, 075320 (2006).
[18] A. H. Castro Neto *et al.* Rev. Mod. Phys. **81**, 109 (2009).
[19] K. Wakabayashi *et al.*, Phys. Rev. B 59, 8271 (1999).
[20] H. Xu *et al.* Phys. Rev. B **77**, 245401 (2008).
[21] A. A. Shylau, J. W. Klos and I. V. Zozoulenko, Phys. Rev. B **80**, 205402 (2009)
[22] P. G. Silvestrov and K. B. Efetov, Phys. Rev. B **77**, 155436 (2008).
[23] J. W. McClure, Phys. Rev. **104**, 666 (1956).
[24] T. Suzuki and T. Ando, Physica B **249–251**, 415 (1998).